Functional and structural characterization of a dense core secretory granule sorting domain from the PC1/3 protease

Jimmy D. Dikeakos[a,b], Paola Di Lello[b], Marie-Josée Lacombe[a], Rodolfo Ghirlando[c], Pascale Legault[b], Timothy L. Reudelhuber[a,1], and James G. Omichinski[b,1]

[a]Laboratory of Molecular Biochemistry of Hypertension, Clinical Research Institute of Montréal, Montréal, QC, Canada H2W 1R7; [b]Department of Biochemistry, Université de Montréal, Montréal, QC, Canada H3C 3J7; and [c]Laboratory of Molecular Biology, National Institute of Diabetes and Digestive and Kidney Diseases, Bethesda, MD 20892

Edited by Donald F. Steiner, University of Chicago, Chicago, IL, and approved March 20, 2009 (received for review September 24, 2008)

Several peptide hormones are initially synthesized as inactive precursors. It is only on entry of these prohormones and their processing proteases into dense core secretory granules (DCSGs) that the precursors are cleaved to generate their active forms. Prohormone convertase (PC)1/3 is a processing protease that is targeted to DCSGs. The signal for targeting PC1/3 to DCSGs resides in its carboxy-terminal tail (PC1/$3_{617–753}$), where 3 regions (PC1/$3_{617–625}$, PC1/$3_{665–682}$, and PC1/$3_{711–753}$) are known to aid in sorting and membrane association. In this article, we have determined a high-resolution structure of the extreme carboxy-terminal sorting domain, PC1/$3_{711–753}$ in micelles by NMR spectroscopy. PC1/$3_{711–753}$ contains 2 alpha helices located between residues 722–728 and 738–750. Functional assays demonstrate that the second helix (PC1/$3_{738–750}$) is necessary and sufficient to target a constitutively secreted protein to granules, and that L^{745} anchors a hydrophobic patch that is critical for sorting. Also, we demonstrate that calcium binding by the second helix of PC1/$3_{711–753}$ promotes aggregation of the domain via the hydrophobic patch centered on L^{745}. These results provide a structure-function analysis of a DCSG-sorting domain, and reveal the importance of a hydrophobic patch and calcium binding in controlling the sorting of proteins containing alpha helices to DCSGs.

NMR | prohormone convertases

Dense core secretory granules (DCSGs) are a repository of proteases and hormones in endocrine and neuroendocrine cells. Many of these proteins are first synthesized as precursors that are activated by protease cleavage after the precursor enters the nascent secretory granules (1–3). The processed proteins are stored within the DCSGs and released when the cell receives the correct stimulus (4). This regulated secretory pathway differs from the pathway of constitutive protein secretion, where proteins are packaged in low-density vesicles and released in an unregulated manner. Thus, the targeting of the protein precursors and their processing enzymes to DCSGs is critical to ensure the secretion of protein hormones such as insulin, glucagon and proteases such as renin.

Two models have been postulated to explain protein sorting to DCSGs (5). The 'sorting by entry' model postulates that proteins are triaged at the trans Golgi network (TGN) via a protein-receptor interaction and proteins interacting with this receptor are diverted into the regulated pathway. A second model is 'sorting by retention' where all proteins, regardless of their final destination, enter an immature secretory granule from which proteins destined for constitutive secretion or targeted to other organelles would be extruded while proteins destined to be stored in the mature DCSG for regulated release would be selectively retained. Nascent granules mature through a process that involves immature granule fusion, acidification, increased calcium content and prohormone processing and condensation (1). Regardless of how DCSG-resident proteins are selected, there must exist a mechanism to accurately sort these proteins to the mature secretory granule.

PC1/3 is one of 3 members of the proprotein/prohormone convertase (PC) family of proteases that has a DCSG-targeted activity (6). PC1/3 requires its carboxy-terminal tail (residues 617–753) to enter DCSGs, and this domain contains three regions (between residues 617–625, 665–682 and 711–753) predicted to form alpha helices that are capable of functioning independently as DCSG sorting signals (7, 8). The signals targeting the related proteases PC2 and PC5/6A to DCSGs have also been reported to be located in the carboxy-terminus (9, 10). Whereas these DCSG-sorting domains have been predicted to form alpha helices based on secondary structure prediction algorithms, there are currently no three-dimensional structures of these domains and thus no information correlating their function to their structure.

In this manuscript, we have determined the NMR solution structure of the PC1/3 DCSG-sorting domain localized at the carboxyl terminus of the protein (residues 711–753). We show that this domain is composed of two amphipathic alpha helices separated by a short eight-residue linker and that the second helix contains a calcium-binding site that promotes aggregation. Functional analysis reveals that the second helix of PC1/$3_{711–753}$ accounts for the DCSG sorting activity and it contains a leucine residue (L^{745}) that anchors a hydrophobic patch that is critical for sorting. The structure in combination with functional experiments in transfected cells help to define how hydrophobic patches in alpha-helical domains mediate protein sorting to DCSGs.

Results

DCSG-Sorting Domain of PC1/3 in a Micellar Environment. We sought to characterize the structure of the PC1/3 domain located between residues 711 and 753 to better understand its ability to sort proteins to DCSGs. A ^{1}H-^{15}N HSQC spectrum of ^{15}N-labeled PC1/$3_{711–753}$ at NMR concentration (1 mM) displayed peak intensity heterogeneity in physiological buffer (Fig. S1*A*) suggesting the presence of line-broadening due to aggregation.

Author contributions: J.D.D., P.D.L., R.G., P.L., T.L.R., and J.G.O. designed research; J.D.D., P.D.L., M.-J.L., R.G., P.L., T.L.R., and J.G.O. performed research; J.D.D., M.-J.L., and R.G. contributed new reagents/analytic tools; J.D.D., P.D.L., M.-J.L., R.G., T.L.R., and J.G.O. analyzed data; and J.D.D., T.L.R., and J.G.O. wrote the paper.

The authors declare no conflict of interest.

This article is a PNAS Direct Submission.

Data deposition: The atomic coordinates and structure factors for PC1/$3_{711–753}$ have been deposited in the Protein Data Bank, www.rcsb.org (PDB ID codes 2ke3 and 2kdt).

[1]To whom correspondence may be addressed. E-mail: reudelt@ircm.qc.ca or jg.omichinski@umontreal.ca.

This article contains supporting information online at www.pnas.org/cgi/content/full/0809576106/DCSupplemental.

www.pnas.org/cgi/doi/10.1073/pnas.0809576106

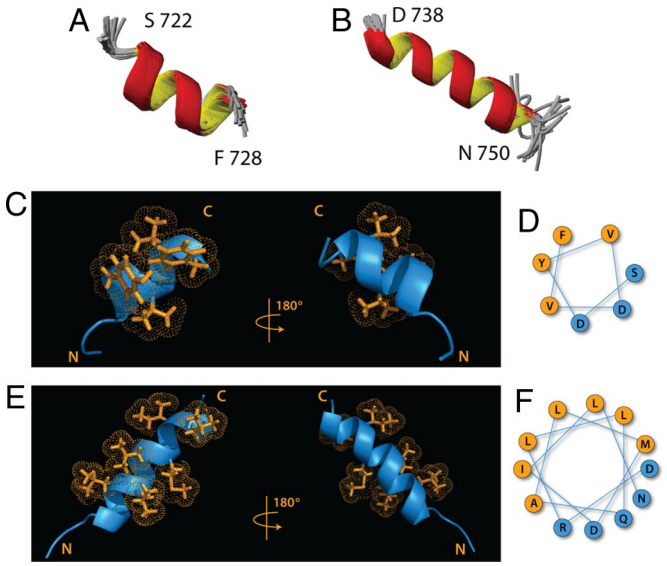

Fig. 1. Structure of PC1/3$_{711–753}$ in CHAPS. The 20 lowest-energy conformers were superimposed using the backbone atoms C′, C$^{\alpha}$, and N of the first helix between residue S^{722} and residue F^{728} (*A*) and the second helix between residue D^{738} and residue N^{750} (*B*). Ribbon (*C* and *E*) and helical wheel (*D* and *F*) representations of the 2 alpha helices in the PC1/3$_{711–753}$ DCSG-sorting domain. Hydrophobic side chains are shown in the ribbon representations, and hydrophobic amino acids are highlighted in orange in the helical wheels while hydrophilic amino acids are represented in blue.

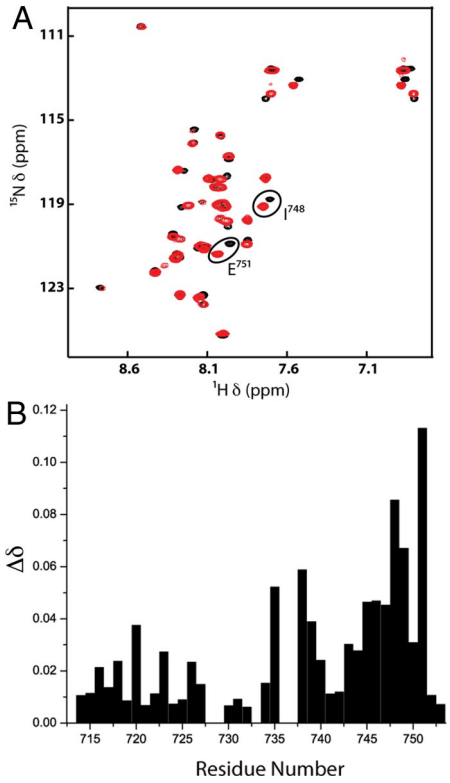

Fig. 2. PC1/3$_{711–753}$ interacts with calcium. (*A*) Overlay of the 2D ^{1}H-^{15}N HSQC spectra of ^{15}N-labeled PC1/3$_{711–753}$ in the free form (black) and in the presence of 10 mM $CaCl_2$ (red). Spectra were recorded in 20 mM d-11 Tris (pH = 6.5) at 26.6 °C with a protein concentration of 1.0 mM in 20 mM CHAPS. Examples of shifted signals are circled. (*B*) Histogram of the variations $\Delta\delta_{(ppm)} = [(0.17\Delta N_H)^2 + (\Delta H_N)^2]^{1/2}$ (39).

Sedimentation velocity experiments (for details, see *SI Materials and Methods*) verified the presence of both high and low molecular weight species at 1 mM PC1/3$_{711–753}$ (Fig. S1*B*). In contrast, a 1 mM sample of ^{15}N-labeled PC1/3$_{711–753}$ in the presence of 20 mM CHAPS (critical micellar concentration = 4–6 mM) gave a homogenous set of NMR signals suggesting that the protein was no longer aggregated (Fig. S1*C*). Identical data were obtained using 200 mM dodecyl phosphocholine (DPC) micelles (Fig. S2). The addition of 20 mM CHAPS or 200 mM DPC to PC1/3$_{711–753}$ at NMR concentrations allowed for the complete ^{1}H, ^{15}N and ^{13}C chemical shift assignment. The use of micelle-forming conditions such as CHAPS and DPC micelles is consistent with previous reports that PC1/3 associates with membranes both in transfected cells (7) and in vitro (8). Thus, NMR structural determination of PC1/3$_{711–753}$ was performed either in the presence of 20 mM CHAPS or 200 mM DPC lipid micelles.

NMR Solution Structure of the PC1/3 DCSG Sorting Domain. A total of 50 conformers was calculated, all of them satisfying the experimental constraints with no NOE violation larger than 0.2 Å and no backbone dihedral angle violation greater then 2°. The 20 conformers with the lowest energies were selected for statistical analysis [20 mM CHAPS (Table S1) and 200 mM DPC (Table S2)]. The NMR solution structures of the DCSG-sorting domain of PC1/3 from residues 711–753 in CHAPS (Fig. 1) and DPC (Fig. S2) indicate the presence of two amphipathic alpha helices located between residues 722–728 and residues 738–750. The angle between the two helices in the sorting domain of PC1/3 could not be defined by NMR due to the absence of long-range NOEs between the two helices. The two amphipathic helices contain both an acidic face and a hydrophobic face. In helix 1 (residues 722–728), the hydrophobic face includes Y^{724}, V^{725}, V^{727} and F^{728}, whereas the hydrophobic face of helix 2 (residues 738–750) includes L^{741}, L^{742}, L^{745}, M^{746}, I^{748} and L^{749}. Interestingly, the second helix (residues 738–750) contains a more prominent hydrophobic patch centered about L^{745}, and this helix overlaps with the region previously predicted to contain a sorting-competent helix (7).

Association of the PC1/3 DCSG-Sorting Domain with Micelles. To identify the residues in the PC1/3$_{711–753}$ domain that are involved in interactions with the CHAPS micelles, we titrated PC1/3$_{711–753}$ with CHAPS (0–20 mM). Quantification of chemical shift pertubation between ^{15}N-labeled PC1/3$_{711–753}$ in the absence of CHAPS and ^{15}N-labeled PC1/3$_{711–753}$ in 20 mM CHAPS allowed us to define two regions of PC1/3$_{711–753}$ displaying significant chemical shift pertubation, and they correspond to residues 724–729 and 741–750 (Fig. S3). These regions coincide with the two alpha helical regions of PC1/3$_{711–753}$ that are located between residues 722–728 and 738–750. In addition, intermolecular NOEs are observed between CHAPS and hydrophobic residues in both the first (V^{725}) and second (L^{741}, L^{742}, L^{745}, M^{746}, and I^{748}) helix. Thus both alpha-helical regions of PC1/3$_{711–753}$ are interacting with membrane-like micelle components.

Identification of a Calcium-Binding Region in PC1/3. It has been proposed that calcium plays a role in sorting based on its high concentration in the DCSGs (10 mM) (3). Divalent cations in the secretory pathway have been reported to induce the aggregation of several proteins that are sorted to DCSGs (11). However, the exact role that calcium plays in sorting of PC1/3 to DCSGs is unknown. To determine if the PC1/3$_{711–753}$ binds calcium, we performed chemical shift mapping studies in the presence of varying concentrations of $CaCl_2$ (1–10 mM). Addition of 10 mM $CaCl_2$ to ^{15}N labeled PC1/3$_{711–753}$ resulted in significant changes in the chemical shifts of several residues of PC1/3$_{711–753}$, as determined by ^{1}H-^{15}N HSQC experiments (Fig. 2*A*). The most

BIOCHEMISTRY

significant chemical shift changes were observed for residues Q^{743}, L^{745}, M^{746}, D^{747} I^{748} and E^{751} (Fig. 2*B*). These residues are present either in the second helix of PC1/$3_{711–753}$ (Q^{743}, L^{745}, M^{746}, D^{747} I^{748}) or in the unstructured region located adjacent to the second helix (E^{751}).

Calcium Binding Promotes Aggregation of the Second Helix of PC1/$3_{711–753}$. To test whether or not calcium plays a role in the aggregation of PC1/$3_{711–753}$, we performed a series of ^{1}H-^{15}N HSQC and sedimentation velocity experiments at low protein concentrations in the absence of micelles. Under these conditions, PC1/$3_{711–753}$ was not aggregated in the absence of calcium ions as verified by both types of experiments (Fig. S4 *A* and *C*). The addition of 10 mM $CaCl_2$ to ^{15}N-labeled PC1/$3_{711–753}$ generated signals with peak intensity heterogeneity in the ^{1}H-^{15}N HSQC spectrum that are consistent with an induction of aggregation by calcium (Fig. S4*B*). The NMR chemical shift assignment of the aggregated PC1/$3_{711–753}$ sample revealed that the amino acids involved in the aggregation are located in the second helix, whereas residues in the first helix of PC1/$3_{711–753}$ gave signals with homogeneous intensity. Further evidence was obtained through sedimentation velocity experiments done in the presence of calcium, where an aggregate species representing 40% of the loading absorbance was observed at 1.8 S (Fig. S4*D*).

Functional Dissection of the PC1/$3_{711–753}$ DCSG Sorting Domain. To determine the relative contribution of the two alpha helices of the PC1/$3_{711–753}$ domain to DCSG sorting, we engineered fusion proteins that attached a constitutively secreted Ig fragment (Fc) (12) to a region containing either the first (PC1/$3_{711–738}$) or second (PC1/$3_{738–753}$) helix. The fusion proteins (FcPC1/$3_{711–738}$ and FcPC1/$3_{738–753}$) were expressed in transfected neuroendocrine AtT20 cells that were pulse-labeled with [^{35}S]-methionine and chased for 16 h in unlabeled medium. Regulated secretion was quantified by comparing the ability of a secretagogue (forskolin) to stimulate the release of radiolabeled fusion proteins that remained in the cells after the overnight chase. In accordance with previous reports, attachment of PC1/$3_{711–753}$ to the Fc fragment causes a dramatic increase in the retention and regulated secretion of the fusion protein by the transfected AtT-20 cells (Fig. 3). The portion of the PC1/3 C-terminal tail containing the first helix (Fc PC1/$3_{711–738}$) did not function as a sorting domain on its own and displayed a sorting ratio comparable to that of Fc fragment alone. In contrast, the residues from 738 to 753 directed the Fc fragment to the regulated secretory pathway with efficiency similar to that of PC1/$3_{711–753}$. These results suggest that the sorting capacity of PC1/$3_{711–753}$ is largely attributable to the second helix located between residues 738 and 750.

To further define the specific amino acids that are responsible for its ability to function as a DCSG sorting signal, we introduced a series of alanine point mutations into the second helix of the FcPC1/$3_{711–753}$ fusion protein (Fig. 4). We first determined the effect of the individual mutations on the ability of the cells to store the proteins in the secretory pathway by comparing the amount of each of the pulse-labeled proteins retained in the cell after a 16 h chase (Fig. 4*A*). Although very little of the labeled Fc protein can be found in the cells after the chase period, linking this protein to the PC1/$3_{711–753}$ domain leads to a dramatic increase in its retention in the cells after an overnight incubation. Although most of the alanine substitutions failed to affect storage, replacing the leucine at position 745 with an alanine (L745A) significantly reduced the storage of the fusion protein, whereas the L749A mutation led to a slight increase in storage. When the fusion proteins were compared for secretion efficiency in response to a secretagogue (Fig. 4 *B* and *C*), both the L742A and L745A substitutions were found to decrease regulated secretion, with the L745A mutation reducing efficiency to a level

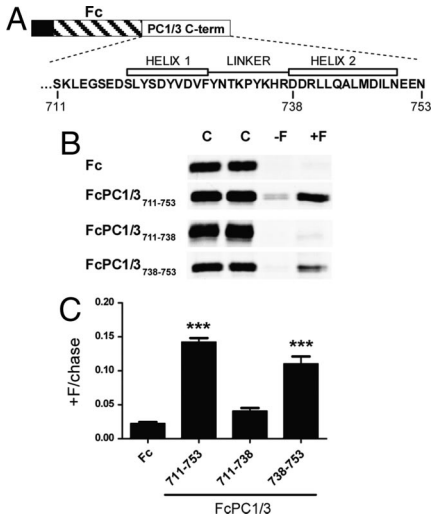

Fig. 3. Functional assay of the two helices in PC1/$3_{711–753}$. (*A*) Schematic diagram of PC1/3 fusion protein fragments used to test for DCSG sorting potential. Proteins are composed of either an Ig fragment (Fc), or Fc fused to PC1/3 peptides containing either both helices (FcPC1/$3_{711–753}$), the first helix and linker region (FcPC$1_{711–738}$) or the second helix (FcPC1/$3_{738–753}$). (*B*) Representative pulse–chase assay for regulated secretion of fusion proteins in AtT-20 cells are shown. For procedure see materials and methods section. Parallel wells of cells are chased for 16 h (C, chase) either in the absence (−F) or in the presence (+F) of the secretagogue forskolin. The relative efficiency of sorting is determined by comparing the amount of protein released by the secretagogue to the amount secreted constitutively in the overnight chase (+F/C). (*C*) Autoradiograms similar to those shown in panel A were exposed to storage phosphor screen and quantified. Shown are the ratios (mean ± SEM) of fusion protein content in the regulated (+F) versus the corresponding overnight chase (C) incubations. $n = 4–6$ independent transfections. ***, $P < 0.001$ as compared with Fc alone.

equivalent to that of the fusion protein in which the entire second helix is deleted (FcPC$1_{711–738}$). Thus, L^{745} is essential for both the intracellular storage and the regulated secretion of fusion proteins containing the PC1/$3_{711–753}$ peptide, consistent with a critical role in the DSCG targeting activity of this domain.

In an attempt to correlate sorting efficiency in transfected cells with aggregation in vitro, we tested whether the PC1/$3_{711–753}$ L745A mutant would aggregate at high protein concentrations (0.25 mM or above) or in the presence of calcium as observed with the native PC1/$3_{711–753}$. A two-dimensional ^{1}H-^{15}N HSQC spectrum of a 0.5 mM ^{15}N-labeled PC1/$3_{711–753}$ L745A mutant gave a homogenous set of signals in the absence or presence of calcium (Fig. S5 *A* and *B*) and sedimentation velocity experiments demonstrated the presence of a single monomeric species in both the absence and presence of calcium (Fig. S5 *C* and *D* and Table S3). Similar results were also obtained with a previously identified sorting-deficient mutant (L745P/L749P) (Fig. S5 *E–H* and Table S3) (7). Thus, the DCSG sorting-deficient mutants of PC1/$3_{711–753}$ fail to aggregate at the same calcium and protein concentrations as the native PC1/$3_{711–753}$, suggesting a correlation between in vitro aggregation mediated by the second helix of PC1/$3_{711–753}$ and its ability to direct sorting to DCSGs.

Discussion

In this manuscript, we have determined the first high-resolution structure of an alpha-helix based DCSG-sorting domain. PC1/$3_{711–753}$ contains two alpha helices separated by a short eight-residue flexible linker. Both helices are amphipathic and contain a hydrophobic face that interacts with the CHAPS and DPC micelles. A phylogenetic comparison (13) reveals that the segment of the PC1/3 C-terminal tail between amino acids 717–749,

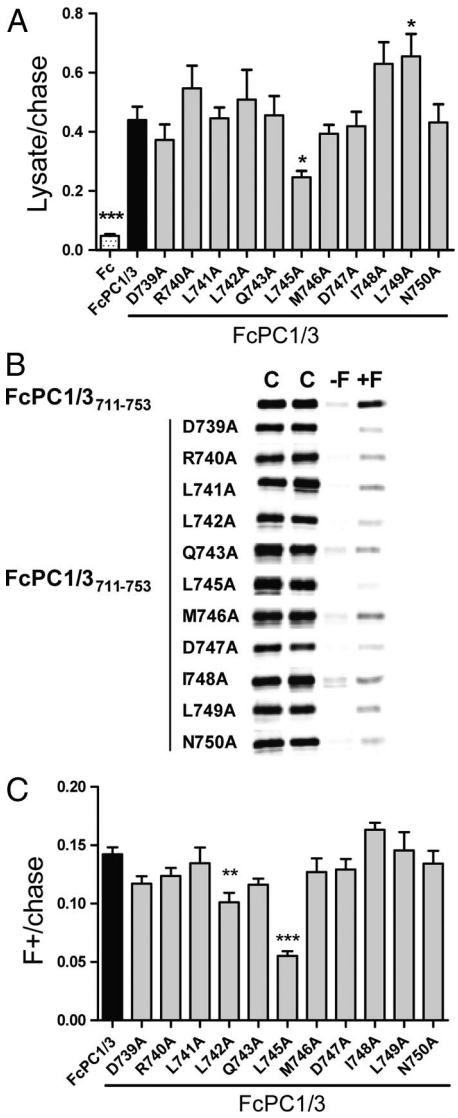

Fig. 4. Site-directed mutagenesis of the second helix of PC1/$3_{711–753}$. Alanine substitution was used to identify residues in the second helix that are functionally important for DCSG sorting. (*A*) AtT-20 cells transfected with the designated alanine-substituted Fc fusion proteins were pulse-labeled with 35-S methionine. After a 16 h chase in unlabeled medium, radiolabeled fusion protein distribution was determined by immunoprecipitation. Shown are the ratios (mean ± SEM) of radiolabeled fusion protein content in cell lysates versus the corresponding overnight chase medium. (*B*) Parallel wells of pulse-labeled transfected AtT-20 cells were tested for regulated secretion of the indicated fusion proteins after a 16 h chase as described in the legend to Fig. 3. (*C*) Shown are the ratios (mean ± SEM) of fusion protein content in the regulated (+F) versus the corresponding overnight chase (C) incubations. n = 4–8, independent transfections. ***, $P < 0.001$; **, $P < 0.01$; *, $P < 0.05$ versus FcPC1/$3_{711–753}$.

a region which encompasses both helices as well as the linker that connects them, is highly conserved from fish to human, raising the possibility that this domain is under some functional selection pressure (Fig. S6*A*).

The interaction of PC1/$3_{711–753}$ with the CHAPS and DPC micelles is consistent with the DCSG-sorting domain being tethered on the membrane surface. There are several reasons to support that this interaction forms the basis of sorting to DCSGs: First, we have previously searched for protein interactions involving the PC1/$3_{711–753}$ domain by in situ protein cross-linking in endocrine cells without success, although self-association was detected (7). Second, we previously reported that sorting-competent versions of PC1/$3_{711–753}$ associate with the membrane fraction in endocrine cells, whereas those unable to sort remain in the soluble fraction of cell lysates (7). Third, we previously reported that several synthetic alpha helices were capable of replacing the natural helix in PC1/$3_{711–753}$ to direct DCSG sorting despite dramatic variations in amino acid composition, making it highly unlikely that hetero-protein–protein interactions are involved (12). This lack of protein homology and the tendency to associate with membranes are also characteristics of other natural helices that direct DCSG sorting (5), making it likely that the biophysical characteristics of the helices play a central role in the association with membranes and the sorting process. Since both helices interact with the micelles through their hydrophobic face and we did not observe interactions between the two helices, it appears that these structural elements interact with the micelle (and the membrane) in a carpet-like mechanism (14), effectively laying on the membrane surface. Interestingly, two similar DCSG-sorting motifs have also been observed in SgII (15). SgII contains both an amino-terminal and a carboxy-terminal sorting domain, and both of these domains have been predicted to form helix–loop–helix motifs. Moreover, in both of these motifs the second helix was necessary and sufficient to direct SgII to granules. The linker region between helices for these sorting domains may ensure that the proteins do not form longer membrane spanning helices that would hinder their subsequent extracellular release.

We also demonstrated that L^{745} in the second helix of PC1/$3_{711–753}$ is a critical hydrophobic residue in mediating the sorting of PC1/3 to granules. A surface representation of PC1/$3_{711–753}$ demonstrates that the protein contains a strong hydrophobic patch in the second helix centered about L^{745} (Fig. S6*B*). Indeed, substitution of an alanine at position 745 is predicted to disrupt the hydrophobic cluster present in the second helix (Fig. S6*B*) and this may explain why the L745A mutation dramatically reduces the sorting efficiency of PC1/$3_{711–753}$. The importance of such a hydrophobic cluster in DCSG sorting is consistent with previous results using synthetic (12) and natural (16) DCSG-sorting helical domains. Likewise, Sar1P contains an amino-terminal helix critical in the targeting of the protein to COP1 coated vesicles (17). Mutational analysis of Sar1p demonstrates that the hydrophobic residues are more important than the alpha-helical structure in the targeting of Sar1p to COP1 vesicles. Recently, it has also been demonstrated that luteinizing hormone is targeted to granules by a non-alpha helical leucine-rich sequence situated at its carboxy-terminus (18). While the authors did not investigate the membrane-binding capability of luteinizing hormone, they did observe that the protein dimerized through its leucine-rich granule-targeting region. Thus, hydrophobic regions may promote both membrane binding as well as formation of high molecular weight complexes that could be tethered to DCSG membranes, preventing their extrusion into constitutively secreted low-density vesicles.

Calcium and divalent metals are present in high concentrations at both the TGN and the DCSGs of endocrine cells (3), and divalent cations have been implicated in the sorting to DCSGs of several proteins including atrial natriuretic factor (19), prolactin and growth hormone (11). It has also been shown that calcium ions can modulate the aggregation state of the highly acidic granule protein chromogranin A (CgA) (20). Calcium binding to CgA results in high-molecular weight complexes which are sorted to DCSGs. In the current study, we identified several residues in the second helix of PC1/$3_{711–753}$ that displayed significant chemical shift pertubation upon the addition of calcium. The addition of calcium also effectively decreased the protein concentration at which the PC1/$3_{711–753}$ domain aggregated in vitro. It is interesting to note that both calcium and lipids interact more strongly with amino acids in the second helix. In

addition, mutation of L^{745} leads to disruption of a strong hydrophobic patch on the surface of the second helix and renders the protein more resistant to calcium-mediated aggregation. Thus, there appears to be a link between the two phenomena, and although our data suggests a correlation between aggregation and DCSG sorting efficiency, the overlap between calcium and lipid binding by the second helix makes it difficult to judge their individual contributions to sorting. In cells, rising calcium levels in the regulated secretory pathway might play one of several roles including the induction of clustering of the PC1/3 DSCG-sorting domains, which could in turn lead to an increase in its local concentration and perhaps its aggregation. Calcium might also neutralize the charges on the second helix and thereby facilitate the interaction of the crucial hydrophobic patch of the sorting domain with membranes. In combination, these effects might improve sorting efficiency by anchoring aggregates of PC1/3 to DCSG membranes.

In summary, we have provided the first high-resolution structure of a DCSG-sorting domain and demonstrated that the second helix of $PC1/3_{711–753}$ is necessary and sufficient for sorting to DCSGs. The structure of $PC1/3_{711–753}$ in conjunction with functional data reveals the importance of a hydrophobic patch centered about L^{745} in mediating this sorting event.

Methods

Protein Purification. Mouse PC1/3 cDNA (NM013628) encoding amino acids 711–753 was inserted in to the pGEX-4T (GE Healthcare) vector and expressed in *E.Coli* Topp2 cells. Cells were grown in 2 L of LB or minimal media containing $^{15}NH_4Cl$ and/or ^{13}C-glucose and induced with IPTG for 3 h at 30 °C. Pellets were resuspended in 100 ml of Buffer A (20 mM Tris, pH = 7.4, 1 M NaCl, 1 mM EDTA and 1 mM DTT) and lysed. Bacterial lysates were centrifuged and the supernatant was incubated with 10 ml of Glutathione-Sepharose resin (GE Healthcare). Bound resin was washed with Buffer A and incubated overnight with thrombin protease (GE Healthcare) in phosphate buffer saline (PBS) to release $PC1/3_{711–753}$. The resulting supernatant was dialyzed against 5% acetic acid and then purified to homogeneity by reverse-phase high pressure liquid chromatography (HPLC) on a C_4 (Vydac) column.

NMR Sample Preparation and Data Collection. For NMR studies, ^{15}N or $^{13}C/^{15}N$ labeled $PC1/3_{711–753}$ peptide was resuspended at a concentration of 1 mM in 20 mM d_{11}-Tris (Cambridge Isotopes) (pH = 6.85) with either 20 mM 3-[(3-cholamidopropyl)dimethylammonio]-1-propanesulfonate (CHAPS) (Fisher) or 200 mM d_{38}-DPC (Cambridge Isotopes) in either 90% H_2O/10% D_2O or 99.9% D_2O. NMR spectra were collected at 300 K on Varian Unity Inova 500 MHz, 600 MHz and 800 MHz NMR spectrometers. The backbone and aliphatic side chain resonances were assigned using two-dimensional (2D) ^1H-^{15}N heteronuclear single quantum coherence (HSQC) (21), 2D ^1H-^{13}C constant-time HSQC (CT-HSQC), 2D HBCBCGCDHD (22), 2D HBCBCGCDCEHE (22), 3D, HNCACB (23), 3D (HB)CBCA(CO)NNH (24), 3D HNCO (25), 3D H(CCO)NNH, 3D (H)C(CO)NNH (24, 25), 3D HNHA (26), and 3D HCCH-correlation spectroscopy (COSY). Intermolecular NOEs between the CHAPS micelle and $^{15}N/^{13}C$-labeled $PC1/3_{711–753}$ were obtained from a 3D $^{15}N/^{13}C$ (F1)-filtered, (F3)-edited nuclear Overhauser effect spectroscopy (NOESY) -HSQC (27). The NMR data were processed with the NMR Pipe/NMRDraw package (28) and analyzed with NMRView (29).

Structure Calculations. The interproton distances were estimated from the intensities of the cross peaks observed in the 3D ^{15}N-edited NOESY-HSQC (30, 31) and ^{13}C-edited heteronuclear multiple quantum coherence-total correlation (HMQC)-NOESY experiments (32). The backbone dihedral angles were obtained from the analysis of ^1H, ^{15}N, $^{13}C'$, $^{13}C^{\alpha}$, and $^{13}C^{\beta}$ chemical shifts using the program TALOS (33). Structure calculations were performed with the program CNS (34) using a combination of torsion angle dynamics (TAD) and Cartesian dynamics. Starting from an extended structure with standard geometry, 50 conformers were calculated and these 50 conformers did not have any NOE violation >0.2 Å and no backbone dihedral angle restraint violation $>2°$. Ramachandran analysis was performed using Procheck (35). Illustrations were prepared with the programs PYMOL (www.pymol.org), Chimera (36) and MOLMOL (37).

Recombinant Plasmid Construction. Peptide fragments to be analyzed for secretory-granule sorting were derived from the mouse PC1/3 cDNA. Protein fragments were tested for their ability to sort a heterologous protein to secretory granules by attachment to a fragment of mouse Ig IgG2b (Fc), as previously described (12). The PC1/3 fusion protein was constructed by selective amplification of corresponding fragments. Mutations were made using PCR overlap extension (38). All of the resulting coding sequences were verified by DNA sequencing and were inserted into the pRSV globin mammalian expression vector (7).

Mammalian Cell Culture, Transfection, and Secretion Analysis. To quantify regulated secretion, stably transfected pools of neuroendocrine AtT20 cells expressing the various fusion proteins were pulse-labeled with [^{35}S]-methionine, chased for 16 h in unlabeled medium and stimulated with a secretagogue to cause secretory granule release as previously described (for details, see *SI Materials and Methods*) (12). To compare DCSG storage of the fusion proteins, stably transfected cells were grown in a 35 mm culture dish, radiolabeled and chased as above. After the 16 h chase period, the cells were rinsed in PBS and the cell monolayers were lysed by addition of 0.5 ml of buffer containing 10 mM Tris (pH 7.5), 1 mM EDTA and 0.1% SDS (TES). After 5 min on ice, the lysate was scraped from the plate and added to 0.5 ml TES with 1% Nonidet P-40. The Fc fusion proteins in the overnight chase medium and the cell lysates were immunoprecipitated and quantified as previously described (12). For statistical analysis, one-way ANOVA with Bonferroni's multiple comparison posttest was performed using GraphPad Prism 5.01 (GraphPad Software, San Diego).

ACKNOWLEDGMENTS. The 800 MHz NMR experiments were recorded at the Québec/Eastern Canada High Field NMR Facility, supported by grants from the Canada Foundation for Innovation and the Québec Ministère de la Recherche en Science et Technologie. This work was supported by the Canadian Institutes of Health Research (CIHR) Grants MOP-135604 (to J.G.O.) and MOP-53177 (to T.L.R.). J.D.D. is a recipient of a studentship from the Fonds de la Recherche en Santé du Québec, and P.D.L. of a fellowship from the CIHR. P.L. is a Canadian Research Chair in Structural Biology of RNA. This work was also supported in part by the Intramural Research Program of the National Institutes of Health, National Institute of Diabetes and Digestive and Kidney Diseases (R.G.).

1. Orci L, et al. (1986) Conversion of proinsulin to insulin occurs coordinately with acidification of maturing secretory vesicles. *J Cell Biol* 103:2273–2281.
2. Taugner R, Kim SJ, Murakami K, Waldherr R (1987) The fate of prorenin during granulopoiesis in epithelioid cells—Immunocytochemical experiments with antisera against renin and different portions of the prorenin prosegment. *Histochemistry* 86:249–253.
3. Schmidt WK, Moore HPH (1995) Ionic milieu controls the compartment specific activation of proopiomelanocortin processing int ATT-20 cells. *Mol Biol Cell* 6:1271–1285.
4. Meldolesi J, Chieregatti E, Malosio ML (2004) Requirements for the identification of dense-core granules. *Trends Cell Biol* 14:13–19.
5. Dikeakos JD, Reudelhuber TL (2007) Sending proteins to dense core secretory granules: Still a lot to sort out. *J Cell Biol* 177:191–196.
6. Seidah NG, Chretien M (1999) Proprotein and prohormone convertases: A family of subtilases generating diverse bioactive polypeptides. *Brain Res* 848:45–62.
7. Jutras I, Seidah NG, Reudelhuber TL (2000) A predicted alpha-helix mediates targeting of the proprotein convertase PC1 to the regulated secretory pathway. *J Biol Chem* 275:40337–40343.
8. Lou H, et al. (2007) The transmembrane domain of the prohormone convertase PC3: A key motif for targeting to the regulated secretory pathway. *Mol Cell Endocrinol* 267:17–25.
9. Creemers JW, et al. (1996) Identification of a transferable sorting domain for the regulated pathway in the prohormone convertase PC2. *J Biol Chem* 271:25284–25291.
10. De Bie I, et al. (1996) The isoforms of proprotein convertase PC5 are sorted to different subcellular compartments. *J Cell Biol* 135:1261–1275.
11. Dannies PS (2002) Mechanisms for storage of prolactin and growth hormone in secretory granules. *Mol Genet Metab* 76:6–13.
12. Dikeakos JD, Lacombe M-J, Mercure C, Mireuta M, Reudelhuber TL (2007) A hydrophobic patch in a charged alpha-helix is sufficient to target proteins to dense core secretory granules. *J Biol Chem* 282:1136–1143.
13. Thompson JD, Higgins DG, Gibson TJ (1994) CLUSTAL-W—Improving the sensitivity of progressive multiple sequence alignment through sequence weighting, position-specific gap penalties and weight matrix choice. *Nucleic Acids Res* 22:4673–4680.
14. Shai Y, Oren Z (2001) From ''carpet'' mechanism to de-novo designed diastereomeric cell-selective antimicrobial peptides. *Peptides* 22:1629–1641.
15. Courel M, Vasquez MS, Hook VY, Mahata SK, Taupenot L (2008) Sorting of the neuroendocrine secretory protein secretogranin II into the regulated secretory pathway—Role of N- and C-terminal alpha-helical domains. *J Biol Chem* 283:11807–11822.
16. Dikeakos JD, Mercure C, Lacombe M-J, Seidah NG, Reudelhuber TL (2007) PC1/3, PC2 and PC5/6A are targeted to dense core secretory granules by a common mechanism. *FEBS J* 274:4094–4102.
17. Lee MCS, et al. (2005) Sar1p N-terminal helix initiates membrane curvature and completes the fission of a COPII vesicle. *Cell* 122:605–617.

18. Jablonka-Shariff A, Pearl CA, Comstock A, Boime I (2008) A carboxyl-terminal sequence in the lutropin beta subunit contributes to the sorting of lutropin to the regulated pathway. *J Biol Chem* 283:11485–11492.
19. Canaff L, Brechler V, Reudelhuber TL, Thibault G (1996) Secretory granule targeting of atrial natriuretic peptide correlates with its calcium-mediated aggregation. *Proc Natl Acad Sci USA* 93:9483–9487.
20. Yoo SH, Albanesi JP (1990) Ca-2+-induced conformational change of aggregation of chromogranin-A. *J Biol Chem* 265:14414–14421.
21. Kay LE, Keifer P, Saarinen T (1992) Pure absorption gradient enhanced heteronuclear single quantum correlation spectroscopy with improved sensitivity. *J Am Chem Soc* 114:10663–10665.
22. Yamazaki T, Formankay JD, Kay LE (1993) 2-dimensional NMR experiments for correlating-13-beta AND H-1-delta/epsilon chemical-shifts of aromatic residues in C-13-labeled proteins via scalar couplings. *J Am Chem Soc* 115:11054–11055.
23. Wittekind M, Mueller L (1993) HNCACB, a high-sensitivity 3D NMR experiment to correlated amide-proton and nitrogen resonances with the alpha-carbon AND beta-carbon resonances in proteins. *J Magn Reson B* 101:201–205.
24. Muhandiram DR, Kay LE (1994) Gradient-enhanced triple-resonance 3-dimensional NMR experiments with improved sensitivity. *J Magn Reson B* 103:203–216.
25. Grzesiek S, Ikura M, Clore GM, Gronenborn AM, Bax A (1992) A 3D triple-resonance NMR technique for qualitatitve measurement of carbonyl-H-beta J couplings in isotopically enriched proteins. *J Magn Reson* 96:215–221.
26. Vuister GW, Wang AC, Bax A (1993) Measurement of 3-bond nitrogen carbon-J couplings in proteins uniformly enriched in N-15 and C-13. *J Am Chem Soc* 115:5334–5335.
27. Zwahlen C, et al. (1997) Methods for measurement of intermolecular NOEs by multinuclear NMR spectroscopy: Application to a bacteriophage lambda N-peptide/boxB RNA complex. *J Am Chem Soc* 119:6711–6721.
28. Delaglio F, et al. (1995) NMRPIPE—A Multidimensional spectral processing system based on UNIX pipes. *J Biomol NMR* 6:277–293.
29. Johnson BA, Blevins RA (1994) NMR VIEW—A computer-program for the visualization and analysis of NMR data. *J Biomol NMR* 4:603–614.
30. Marion D, et al. (1989) Overcoming the overlap problem in the assignment of H-1-NMR spectra of larger proteins by use of 3-dimensional heteronuclear H-1-N-15 Hartmann-Hahn multiple quantum coherence and nuclear overhauser multiple quantum coherence spectroscopy- Application to interleukin-1-beta. *Biochemistry* 28:6150–6156.
31. Marion D, Kay LE, Sparks SW, Torchia DA, Bax A (1989) 3-dimensional heteronuclear NMR of N-15-labeled proteins. *J Am Chem Soc* 111:1515–1517.
32. Zuiderweg ERP, McIntosh LP, Dahlquist FW, Fesik SW (1990) 3-dimensional C-13-resolved proton NOE spectroscopy of uniformly C-13-labeled proteins for the NMR assignment and structure determination of larger molecules. *J Magn Reson* 86:210–216.
33. Cornilescu G, Delaglio F, Bax A (1999) Protein backbone angle restraints from searching a database for chemical shift and sequence homology. *J Biomol NMR* 13:289–302.
34. Brunger AT, et al. (1998) Crystallography & NMR system: A new software suite for macromolecular structure determination. *Acta Crystallogr D* 54:905–921.
35. Laskowski RA, Rullmann JAC, MacArthur MW, Kaptein R, Thornton JM (1996) AQUA and PROCHECK-NMR: Programs for checking the quality of protein structures solved by NMR. *J Biomol NMR* 8:477–486.
36. Pettersen EF, et al. (2004) UCSF chimera—A visualization system for exploratory research and analysis. *J Comput Chem* 25:1605–1612.
37. Koradi R, Billeter M, Wuthrich K (1996) MOLMOL: A program for display and analysis of macromolecular structures. *J Mol Graphics* 14:51–55.
38. Higuchi R, Krummel B, Saiki RK (1988) A general-method of in vitro preparation and specific mutagenesis of DNA fragments—Study of protein and DNA interactions. *Nucleic Acids Res* 16:7351–7367.
39. Farmer BT (1996) Localizing the NADP(+) binding site on the MurB enzyme by NMR. *Nat Struct Biol* 3:995–997.